Remote Floating-Gate Field-effect Transistor with 2-Dimensional Reduced Graphene Oxide Sensing Layer for Reliable Detection of SARS-CoV-2 Spike Proteins

Hyun-June Jang[1,2], Xiaoyu Sui[1,2], Wen Zhuang[1], Xiaodan Huang[1], Min Chen[1], Xiaolei Cai[1], Yale Wang[3], Byunghoon Ryu[2], Haihui Pu[1,2], Nicholas Ankenbruck[1], Kathleen Beavis[4], Jun Huang[1], Junhong Chen[1,2*]

[1]Pritzker School of Molecular Engineering, University of Chicago, Chicago, IL 60637, USA

[2]Chemical Sciences and Engineering Division, Physical Sciences and Engineering Directorate, Argonne National Laboratory, Lemont, IL 60439, USA

[3]Department of Mechanical Engineering, University of Wisconsin-Milwaukee, Milwaukee, WI 53211, USA

[4]Department of Pathology, University of Chicago, Chicago, IL 60637, USA

Corresponding author

*E-mail: junhongchen@uchicago.edu

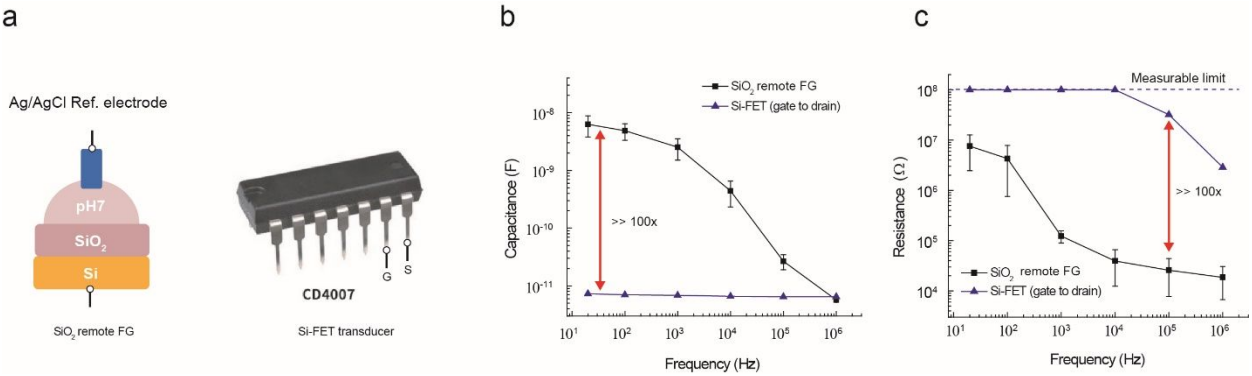

Figure S1. (a) Schematic images of device structure for impedance measurement of remote FG and commercial FET (CD4007). Frequency vs (b) capacitance and (c) resistance of a 300-nm-thick SiO_2 and gate-drain of Si-FET chip. For measurement of remote FG, 50 µL pH7 solution was added on the top of SiO_2 surface. AC frequency was applied through the Ag/AgCl reference electrode and the bottom silicon electrode of each FG. The level of voltage set at 1 V during capacitance and resistance measurement. The input impedance of Si-FET is much higher than those of remote SiO_2 FG, meaning that the effect of impedance of FGs on total impedance of remote FGFET is insignificant.

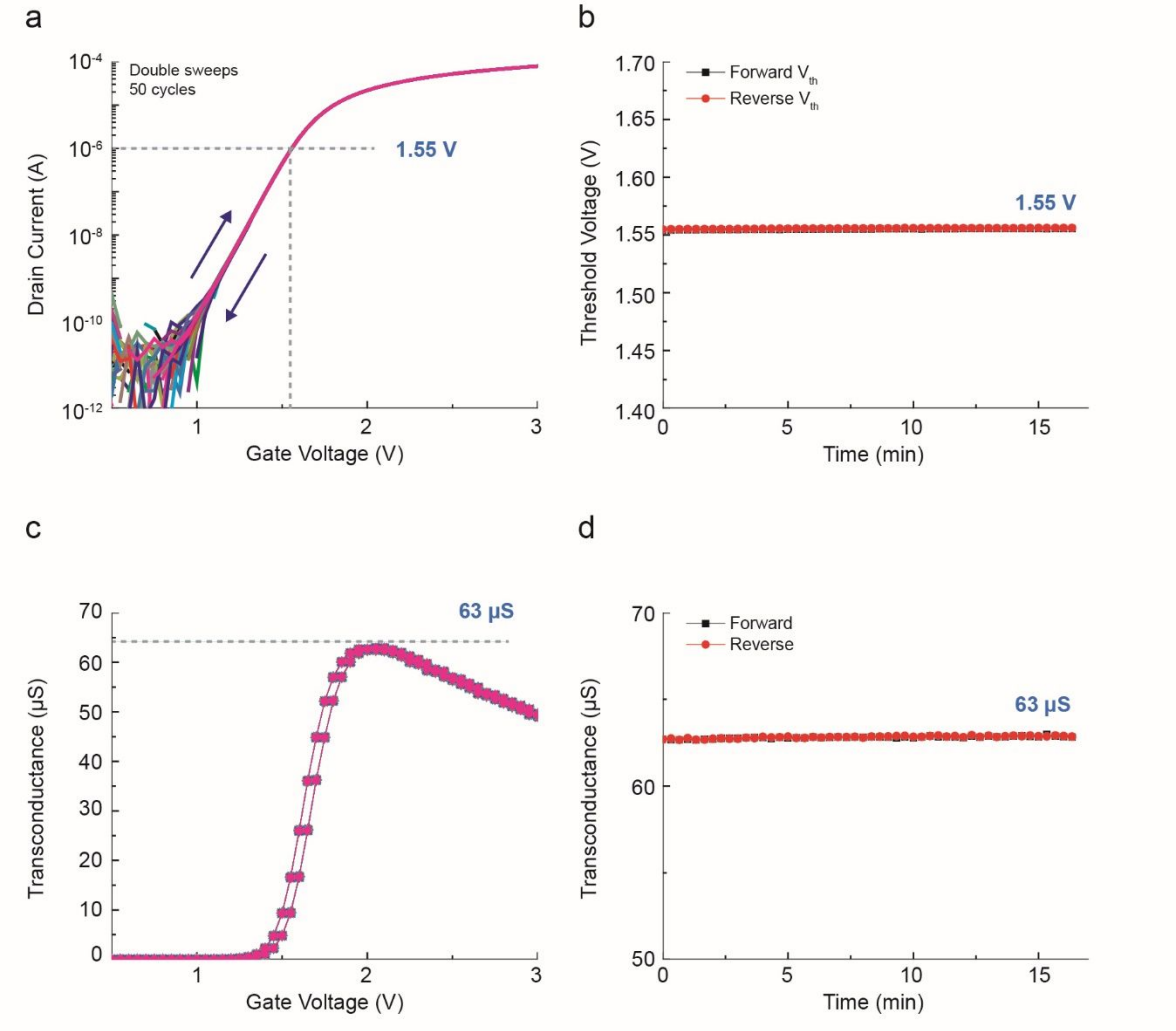

Figure S2. (a) Zoomed-in representative transfer curves of Si-FET with the double-sweeping mode the gate voltage (V_G) ranging from 0 to 5 V for 50 cycles of transfer curves. (b) V_{th} of the MOSFET measured by each forward- and reverse-sweeping mode over time. (c) Representative transconductance (G_m) curves of Si-FET with the double-sweeping mode at the V_G ranging from 0 to 5 V for 50 cycles of transconductance curves. (d) G_m of the MOSFET measured by each forward- and reverse-sweeping mode over time.

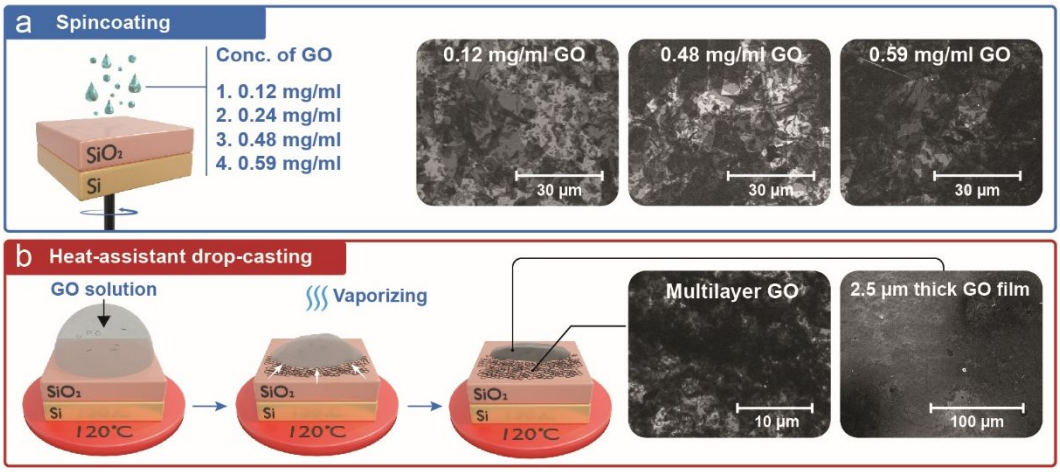

Figure S3. SEM images of GO layers (a) spin-coated with 0.12, 0.48, and 0.59 mg/ml GO solutions and (b) made by a heat-assisted drop-casting method.

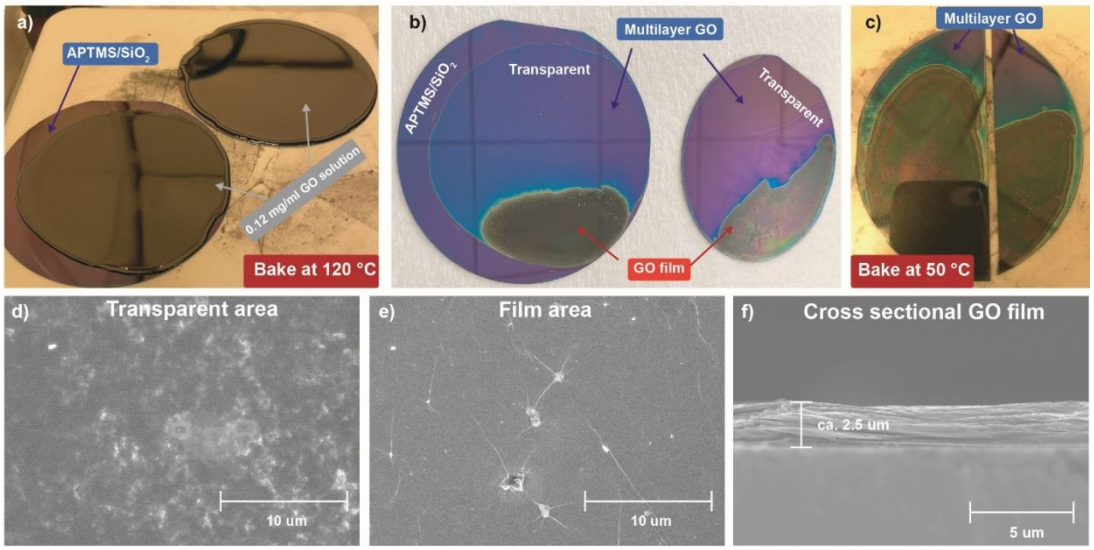

Figure S4. Images of GO films made using the heat-assistant drop-casting method: 0.12 mg/ml GO solution dropped on the APTMS/SiO_2 substrate (a) before and (b) after baking at 120 °C for 1 hour. The lower baking temperature at 50 °C allowed the GO film (dark area) to develop on more areas of the wafer (**Figure S4c**) due to the low evaporation rate of the GO solvent. For the dried wafers, transparent and dark areas appeared on the same APTMS/SiO_2 surface from multilayer GO (**Figure S4d**) and continuous thick GO films (**Figure S4e**), respectively. The thickness of the GO film was measured to be about 2.5 μm for cross-sectional SEM images of the GO film (**Figure S4f**).

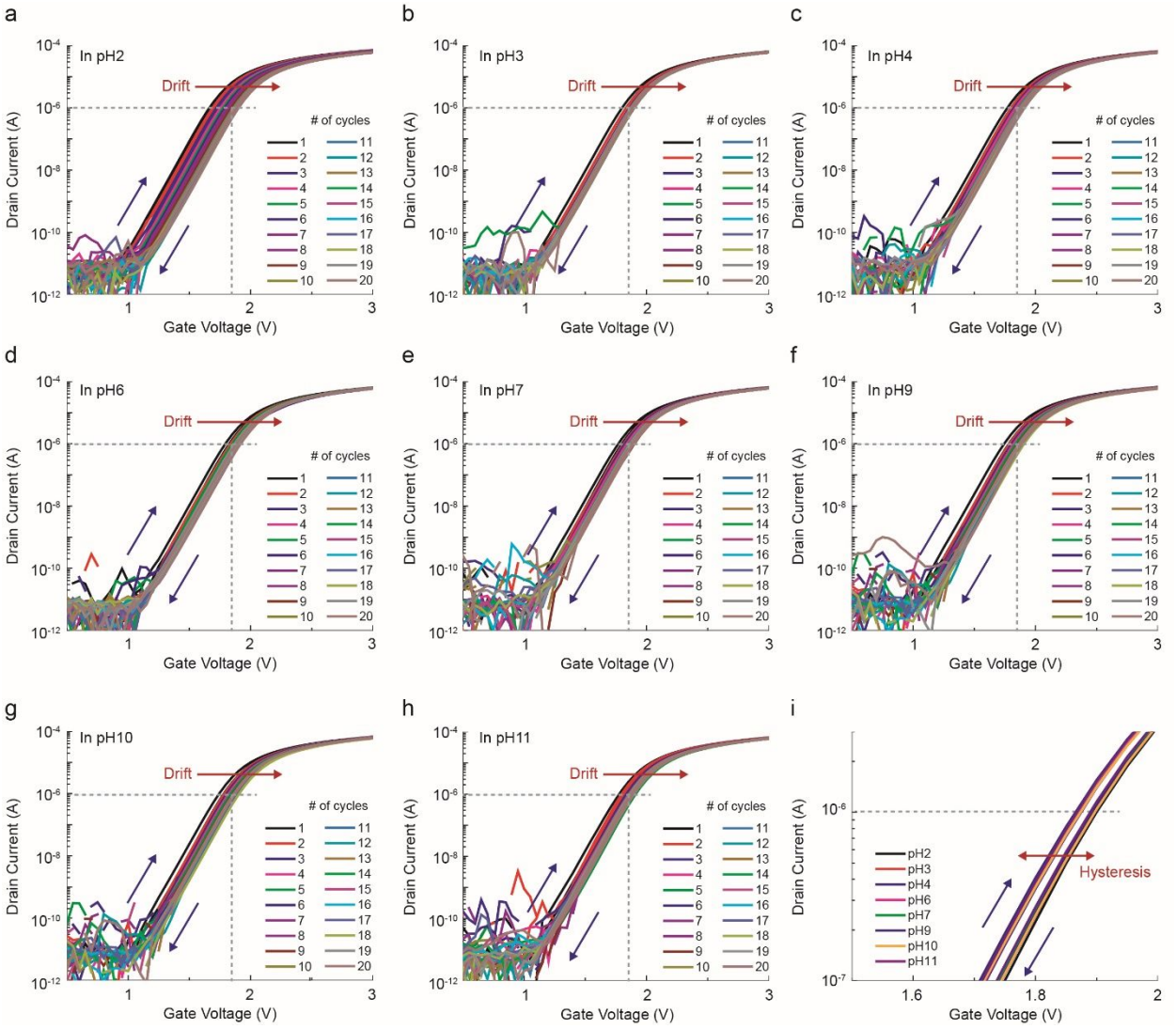

Figure S5. Representative transfer curves of the SiO_2 remote FGFET measured in (a) pH2, (b) pH3, (c) pH4, (d) pH6, (e) pH7, (f) pH9, (g) pH10, and (h) pH11 solution. Transfer curves were measured 20 times for each pH solution under the double-sweep mode with a gate voltage ranging from 0 to 5 V. The drain voltage sets at 50 mV over all measurements. Each initial transfer curve for the respective pH value drifted to the direction on the right with a saturation point. (i) Transfer curves at saturation for each pH solution. The transfer curves mostly overlapped in quasi-equilibrium regardless of pH changes.

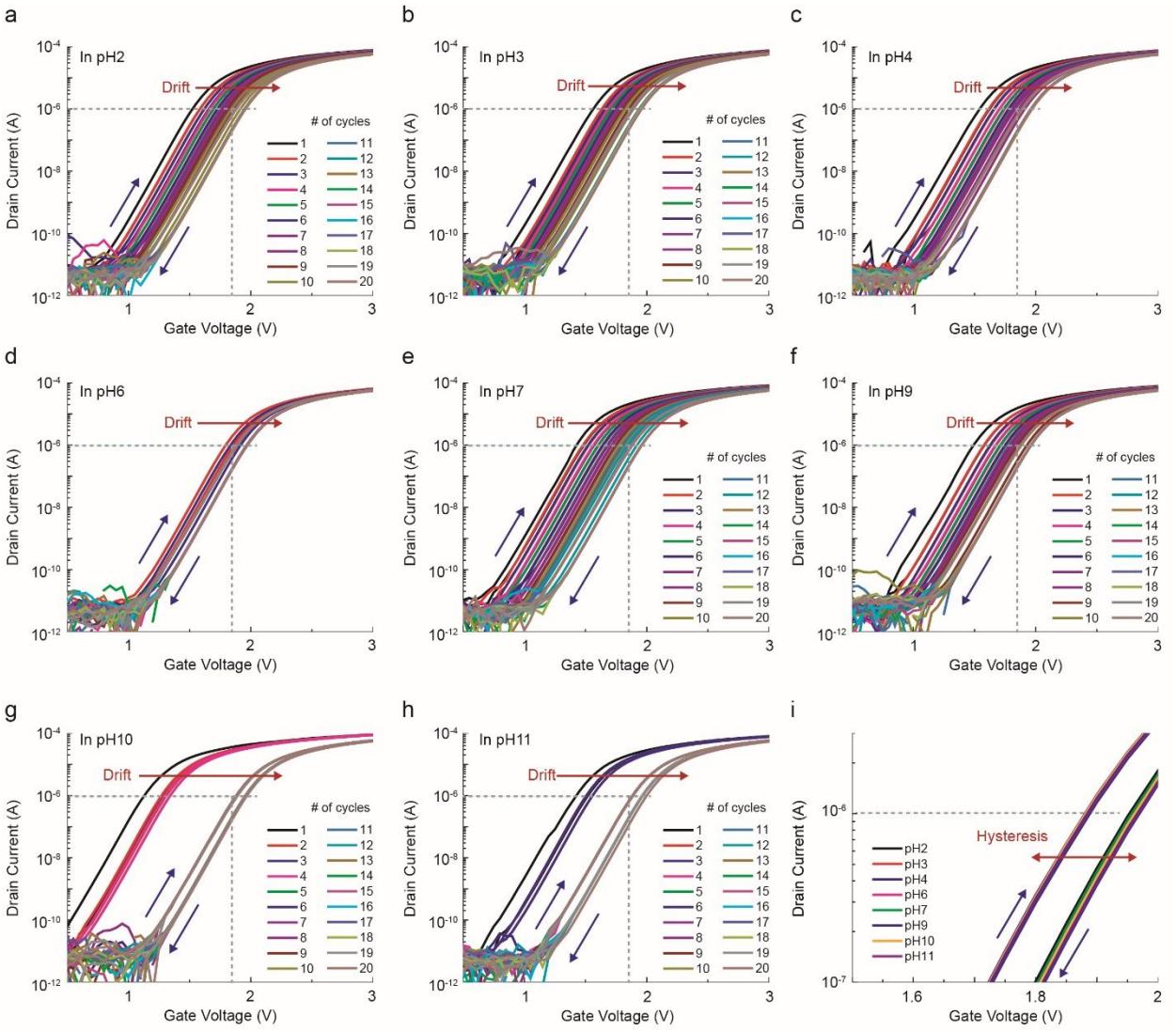

Figure S6. Representative transfer curves of APTMS/SiO_2 remote FGFET measured in (a) pH2, (b) pH3, (c) pH4, (d) pH6, (e) pH7, (f) pH9, (g) pH10, and (h) pH11 solution. Transfer curves were measured 20 times for each pH solution under the double-sweep mode with a gate voltage ranging from 0 to 5 V. The drain voltage sets at 50 mV over all measurements. Each initial transfer curve for the respective pH value drifted to the direction on the right with a saturation point. (i) Transfer curves at saturation for each pH solution. The transfer curves mostly overlapped in quasi-equilibrium regardless of pH changes.

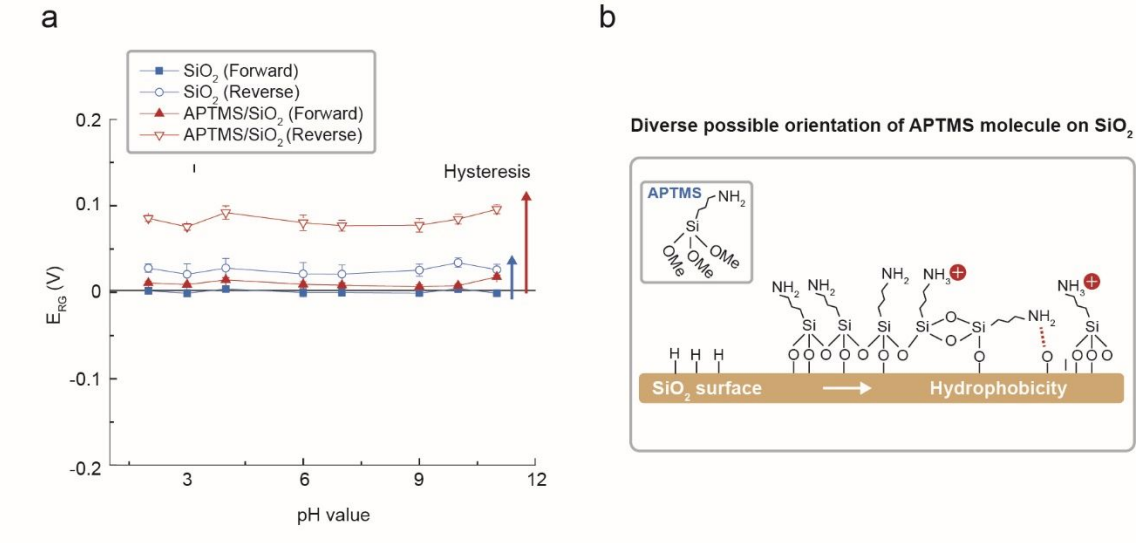

Figure S7. (a) The E_{RG}^{For} and E_{RG}^{Rev} of SiO_2 and APTMS/SiO_2 in quasi-equilibrium vs. pH value. (b) Schematic images of possible APTMS orientations enabling more hydrophobic surfaces than SiO_2.

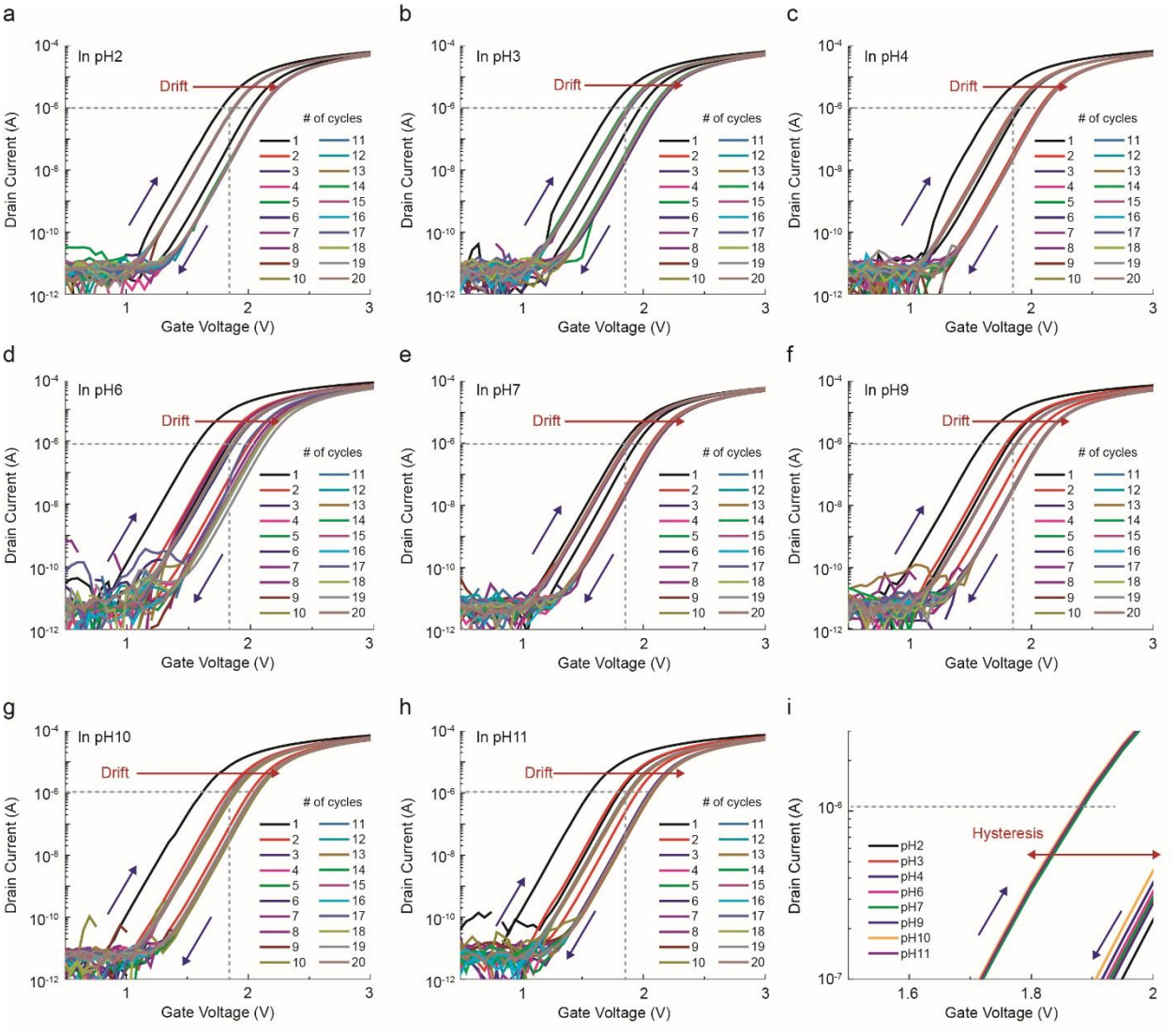

Figure S8. Representative transfer curves of the remote FGFET with a FG surface of spin-coated GO (0.12 mg/ml GO) without post-annealing, which was measured in (a) pH2, (b) pH3, (c) pH4, (d) pH6, (e) pH7, (f) pH9, (g) pH10, and (h) pH11 solution. Transfer curves were measured 20 times for each pH solution under the double-sweep mode with a gate voltage ranging from 0 to 5 V. The drain voltage sets at 50 mV over all measurements. Each initial transfer curve for the respective pH value drifted to the direction on the right with a saturation point. (i) Transfer curves at saturation for each pH solution. The transfer curves mostly overlapped in quasi-equilibrium regardless of pH changes.

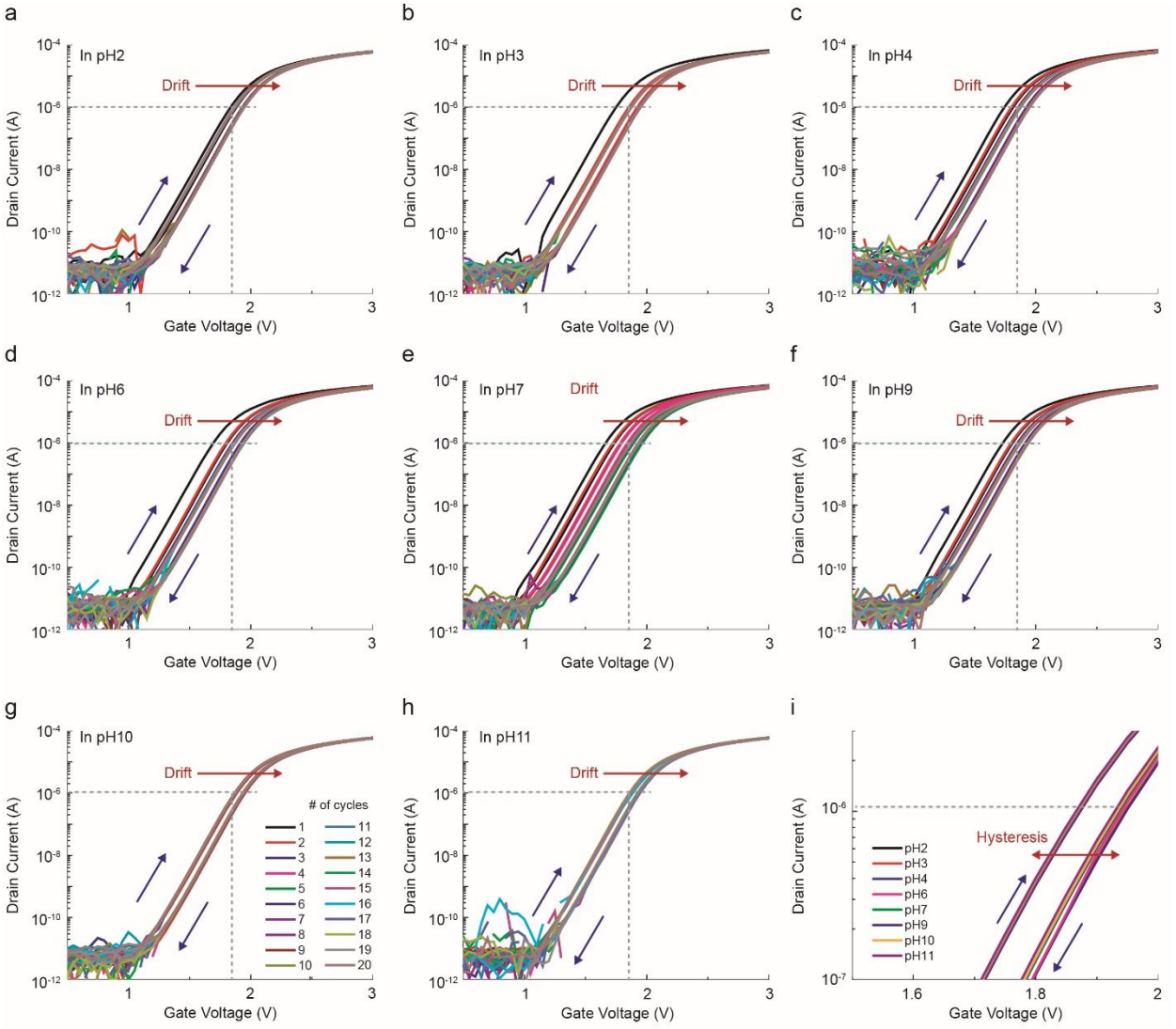

Figure S9. Representative transfer curves of the remote FGFET with a FG surface of spin-coated GO (0.59 mg/ml GO) without post-annealing, which was measured in (a) pH2, (b) pH3, (c) pH4, (d) pH6, (e) pH7, (f) pH9, (g) pH10, and (h) pH11 solution. Transfer curves were measured 20 times for each pH solution under the double-sweep mode with a gate voltage ranging from 0 to 5 V. The drain voltage sets at 50 mV over all measurements. Each initial transfer curve for the respective pH value drifted to the direction on the right with a saturation point. (i) Transfer curves at saturation for each pH solution. The transfer curves mostly overlapped in quasi-equilibrium regardless of pH changes.

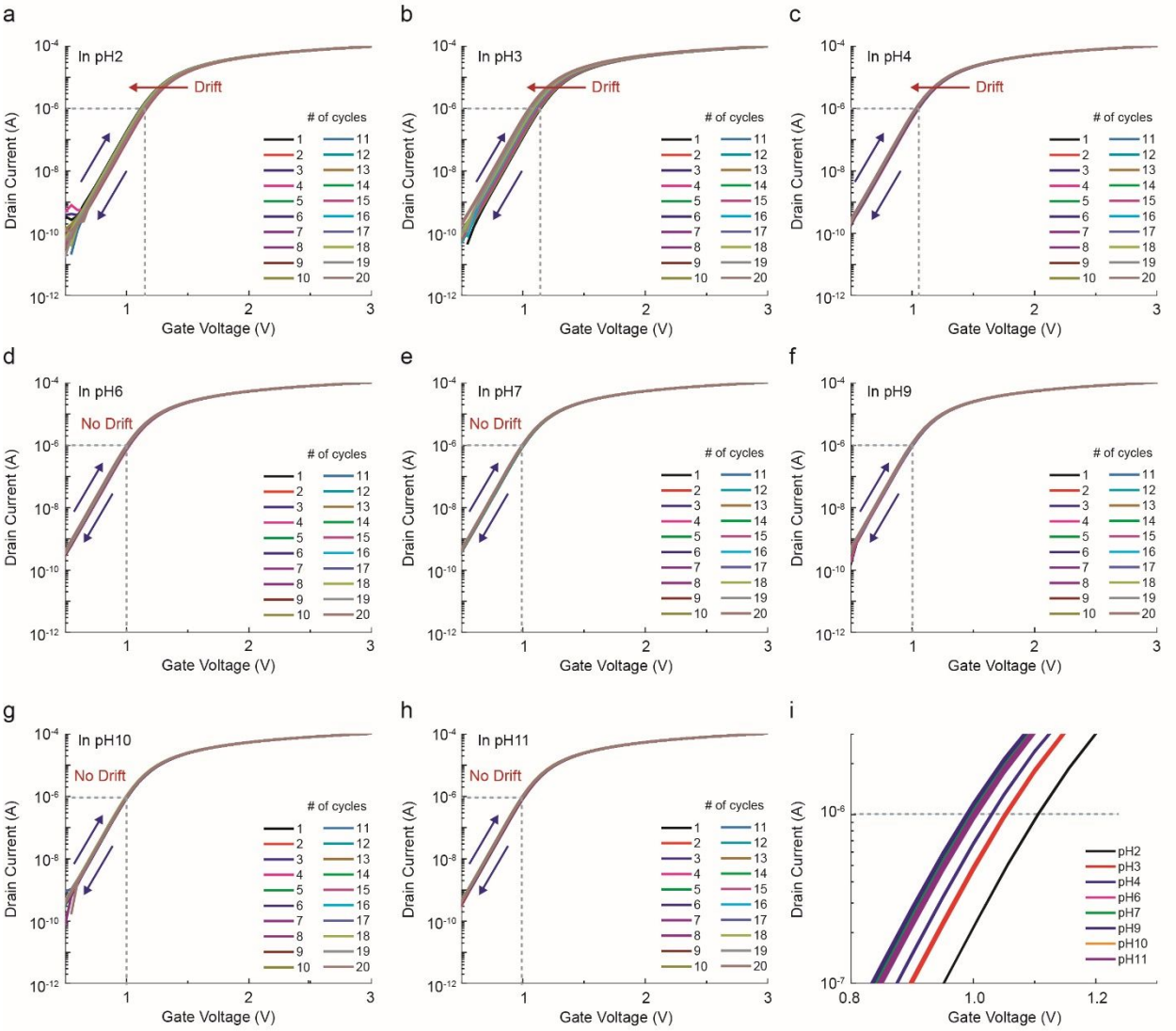

Figure S10. Representative transfer curves of the remote FGFET with a FG surface of drop-casted 2.5 μm GO without post-annealing, which was measured in (a) pH2, (b) pH3, (c) pH4, (d) pH6, (e) pH7, (f) pH9, (g) pH10, and (h) pH11 solution. Transfer curves were measured 20 times for each pH solution under the double-sweep mode with a gate voltage ranging from 0 to 5 V. The drain voltage sets at 50 mV over all measurements. Each initial transfer curve for the respective pH value drifted to the direction on the right with a saturation point. (i) Transfer curves at saturation for each pH solution. The transfer curves mostly overlapped in quasi-equilibrium regardless of pH changes.

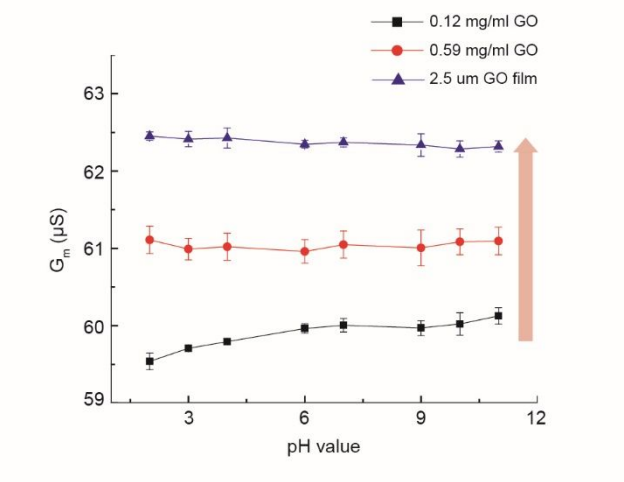

Figure S11. G_m^{For} distributions of 0.12 mg/ml GO films, 0.59 mg/ml GO films, and drop-casted 2.5 μm GO films without reduction process over at least four samples as a function of increasing pH.

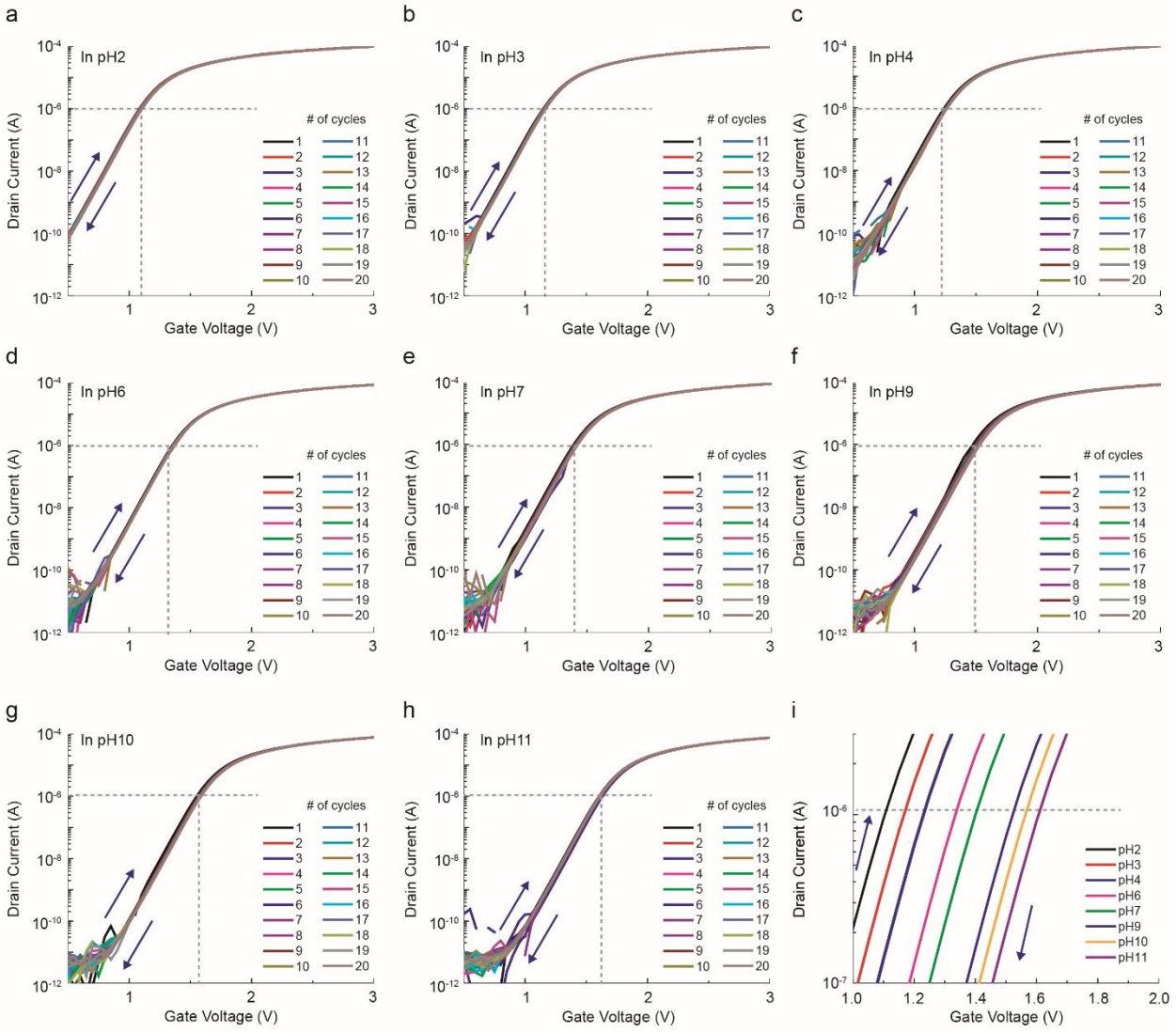

Figure S12. Representative transfer curves of the remote FGFET with a 0.59 mg/ml GO FG surface reduced at 200 °C, which was measured in (a) pH2, (b) pH3, (c) pH4, (d) pH6, (e) pH7, (f) pH9, (g) pH10, and (h) pH11 solution. Transfer curves were measured 20 times for each pH solution under the double-sweep mode with a gate voltage ranging from 0 to 5 V. The drain voltage sets at 50 mV over all measurements. Each initial transfer curve for the respective pH value drifted to the direction on the right with a saturation point. (i) Transfer curves at saturation for each pH solution. The transfer curves mostly overlapped in quasi-equilibrium regardless of pH changes.

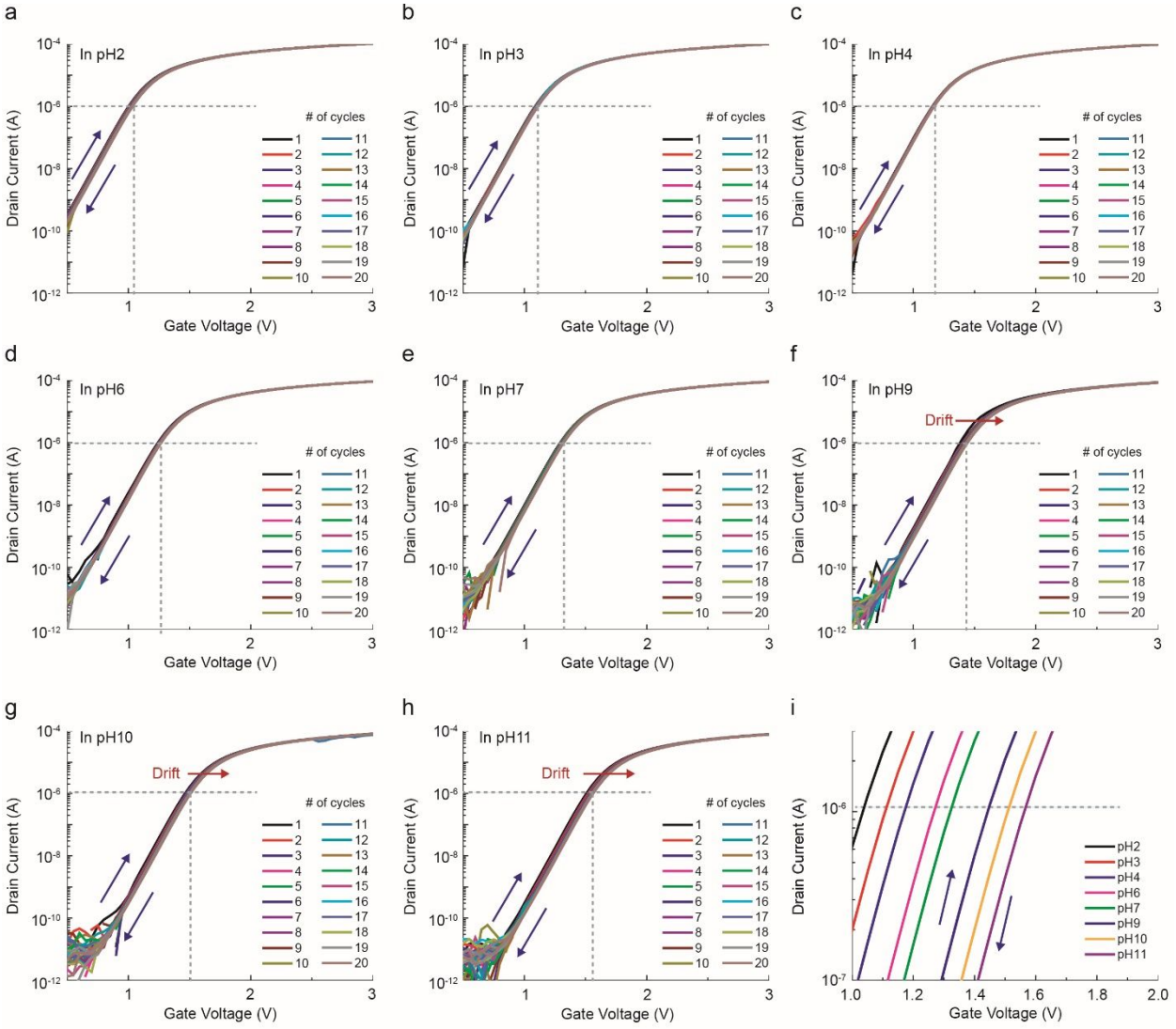

Figure S13. Representative transfer curves of the remote FGFET with a 0.59 mg/ml GO FG surface reduced at 300 °C, which was measured in (a) pH2, (b) pH3, (c) pH4, (d) pH6, (e) pH7, (f) pH9, (g) pH10, and (h) pH11 solution. Transfer curves were measured 20 times for each pH solution under the double-sweep mode with a gate voltage ranging from 0 to 5 V. The drain voltage sets at 50 mV over all measurements. Each initial transfer curve for the respective pH value drifted to the direction on the right with a saturation point. (i) Transfer curves at saturation for each pH solution. The transfer curves mostly overlapped in quasi-equilibrium regardless of pH changes.

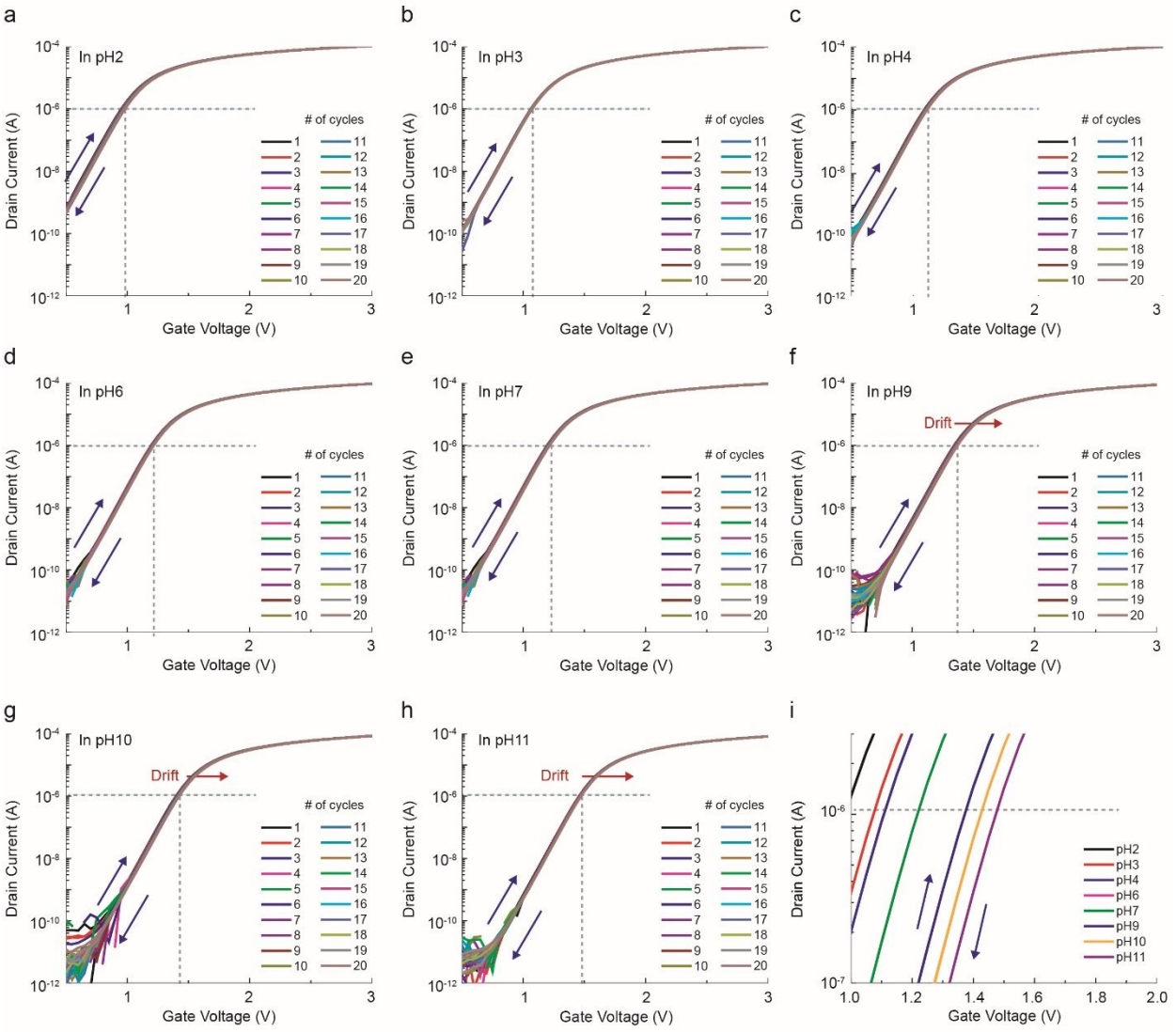

Figure S14. Representative transfer curves of the remote FGFET with a 0.59 mg/ml GO FG surface reduced at 400 °C, which was measured in (a) pH2, (b) pH3, (c) pH4, (d) pH6, (e) pH7, (f) pH9, (g) pH10, and (h) pH11 solution. Transfer curves were measured 20 times for each pH solution under the double-sweep mode with a gate voltage ranging from 0 to 5 V. The drain voltage sets at 50 mV over all measurements. Each initial transfer curve for the respective pH value drifted to the direction on the right with a saturation point. (i) Transfer curves at saturation for each pH solution. The transfer curves mostly overlapped in quasi-equilibrium regardless of pH changes.

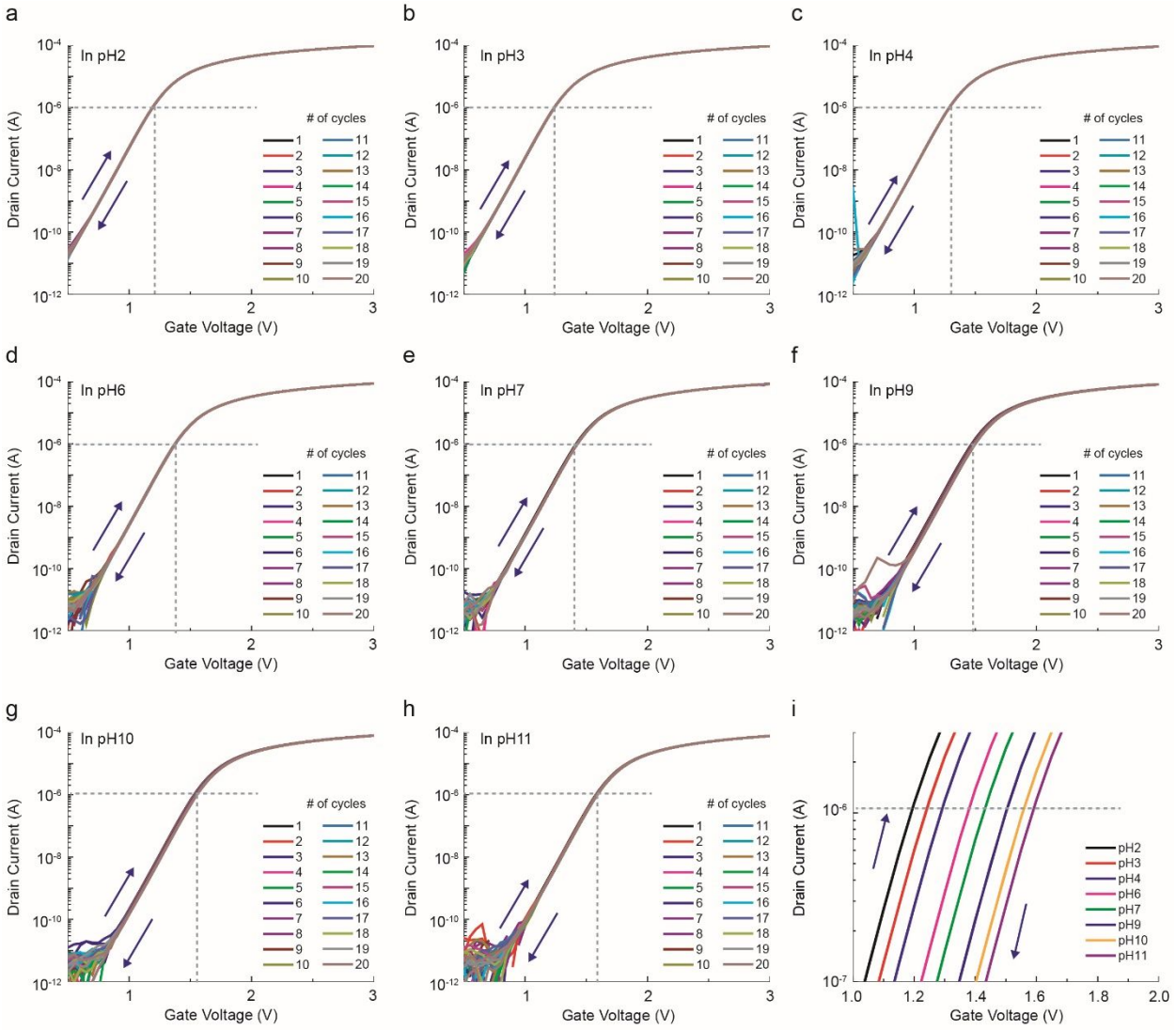

Figure S15. Representative transfer curves of the remote FGFET with the FG surface of 2.5 μm GO reduced at 200 °C, which was measured in (a) pH2, (b) pH3, (c) pH4, (d) pH6, (e) pH7, (f) pH9, (g) pH10, and (h) pH11 solution. Transfer curves were measured 20 times for each pH solution under the double-sweep mode with a gate voltage ranging from 0 to 5 V. The drain voltage sets at 50 mV over all measurements. Each initial transfer curve for the respective pH value drifted to the direction on the right with a saturation point. (i) Transfer curves at saturation for each pH solution. The transfer curves mostly overlapped in quasi-equilibrium regardless of pH changes.

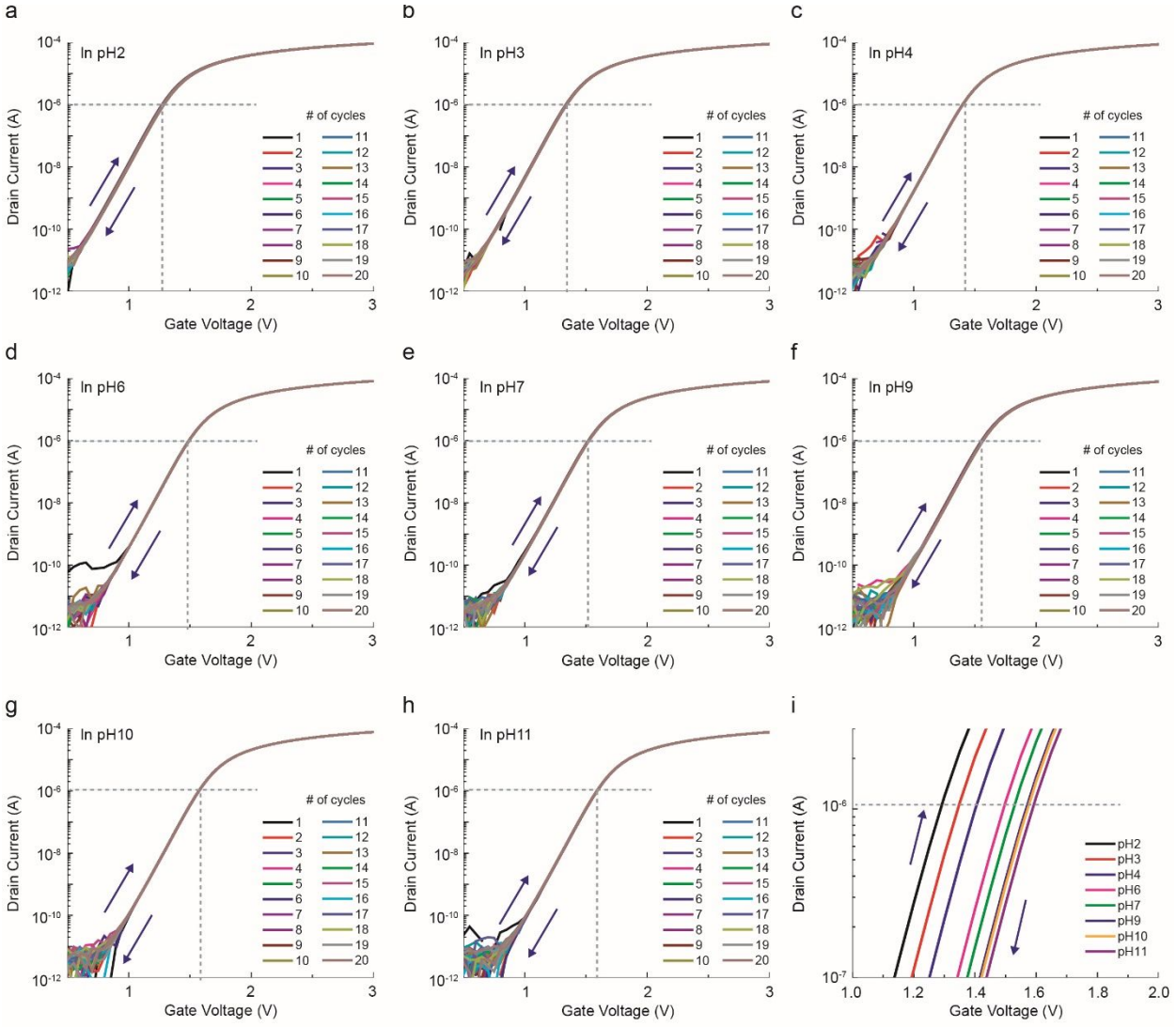

Figure S16. Representative transfer curves of the remote FGFET with the FG surface of 2.5 μm GO reduced at 300 °C, which was measured in (a) pH2, (b) pH3, (c) pH4, (d) pH6, (e) pH7, (f) pH9, (g) pH10, and (h) pH11 solution. Transfer curves were measured 20 times for each pH solution under the double-sweep mode with a gate voltage ranging from 0 to 5 V. The drain voltage sets at 50 mV over all measurements. Each initial transfer curve for the respective pH value drifted to the direction on the right with a saturation point. (i) Transfer curves at saturation for each pH solution. The transfer curves mostly overlapped in quasi-equilibrium regardless of pH changes.

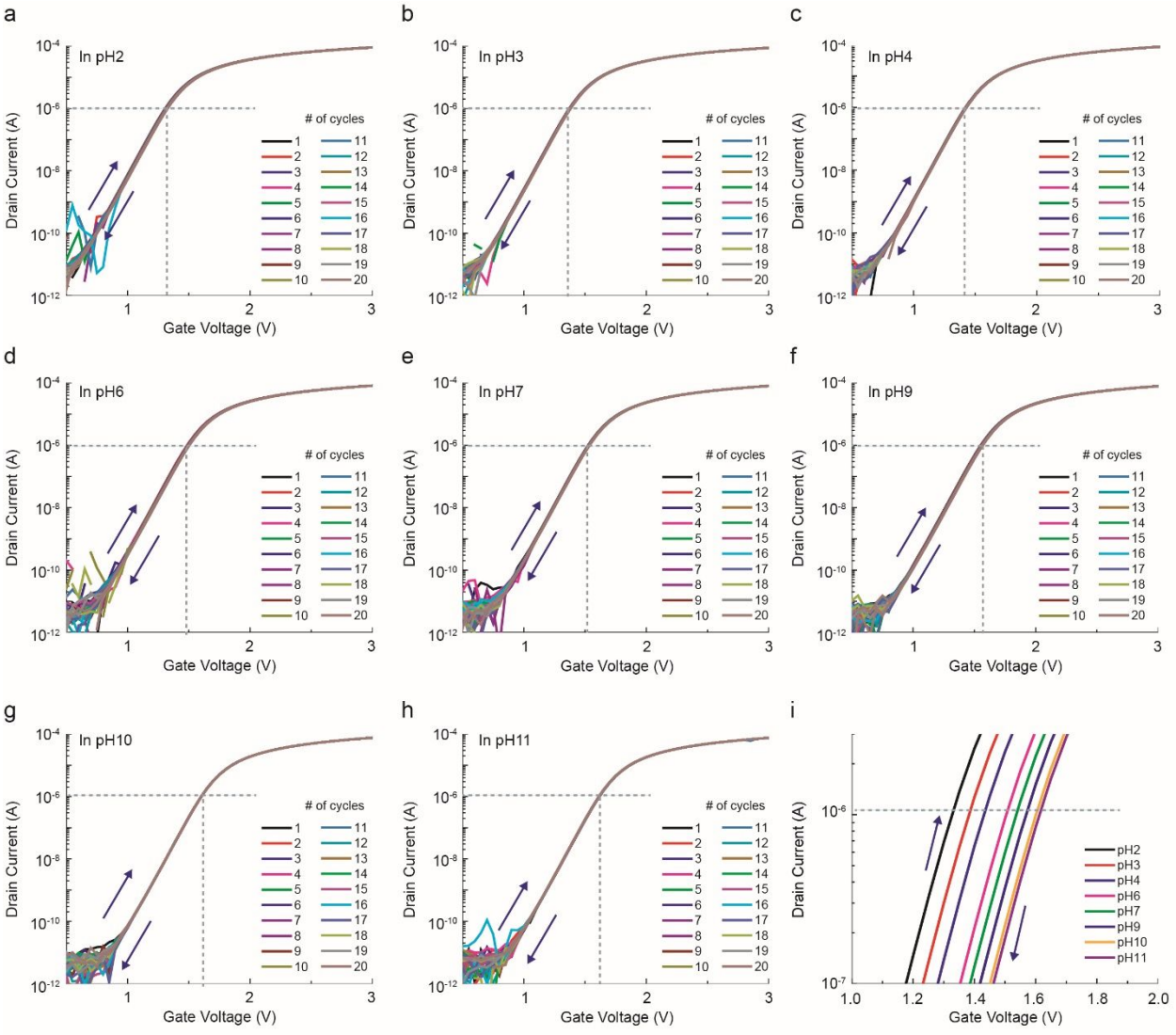

Figure S17. Representative transfer curves of the remote FGFET with the FG surface of 2.5 μm GO reduced at 400 °C, which was measured in (a) pH2, (b) pH3, (c) pH4, (d) pH6, (e) pH7, (f) pH9, (g) pH10, and (h) pH11 solution. Transfer curves were measured 20 times for each pH solution under the double-sweep mode with a gate voltage ranging from 0 to 5 V. The drain voltage sets at 50 mV over all measurements. Each initial transfer curve for the respective pH value drifted to the direction on the right with a saturation point. (i) Transfer curves at saturation for each pH solution. The transfer curves mostly overlapped in quasi-equilibrium regardless of pH changes.

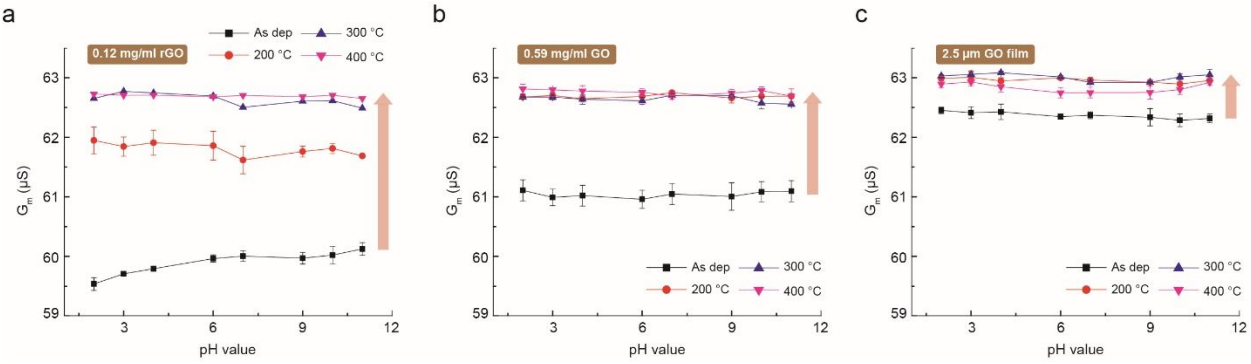

Figure S18. G_m^{For} distributions of (a) 0.12 mg/ml GO films, (b) 0.59 mg/ml GO films, and (c) drop-casted 2.5 μm GO films over at least four samples as a function of increasing pH and reduction temperatures ranging from 200 to 400 °C.

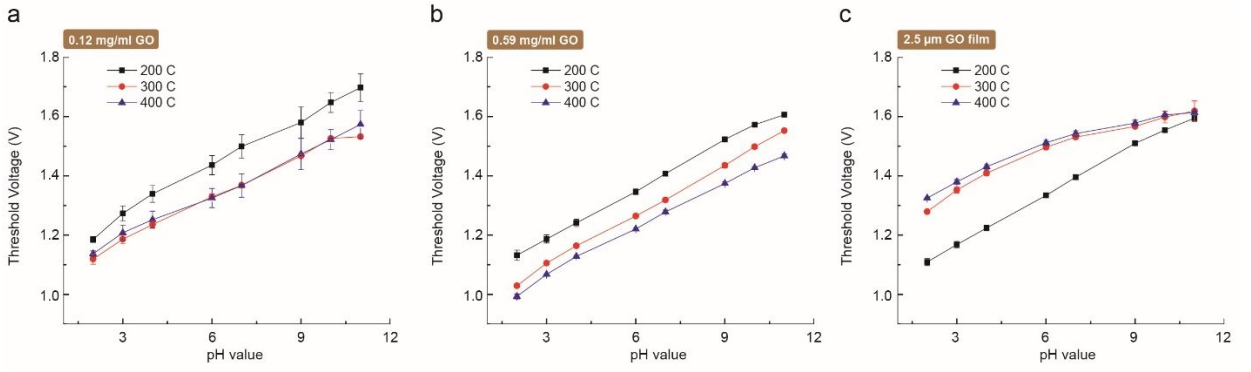

Figure S19. V_{th} distributions from (a) an FG surface with 0.12 mg/ml GO films, (b) 0.59 mg/ml GO films, and (c) drop-casted 2.5 μm GO films over at least three samples as a function of increasing pH and reduction temperatures ranging from 200 to 400 °C.

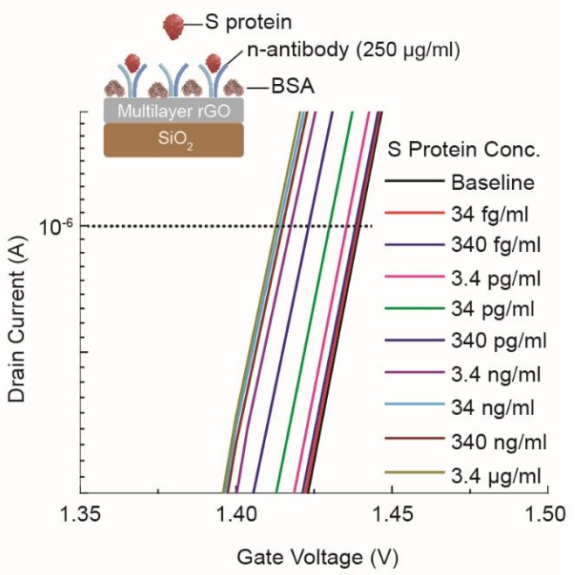

Figure S20. Responses of transfer curves of antibody-functionalized rGO (250 µg/ml antibody) with increasing concentrations of S protein in a range from 34 fg/ml to 3.4 µg/ml in 0.05 × PBS.

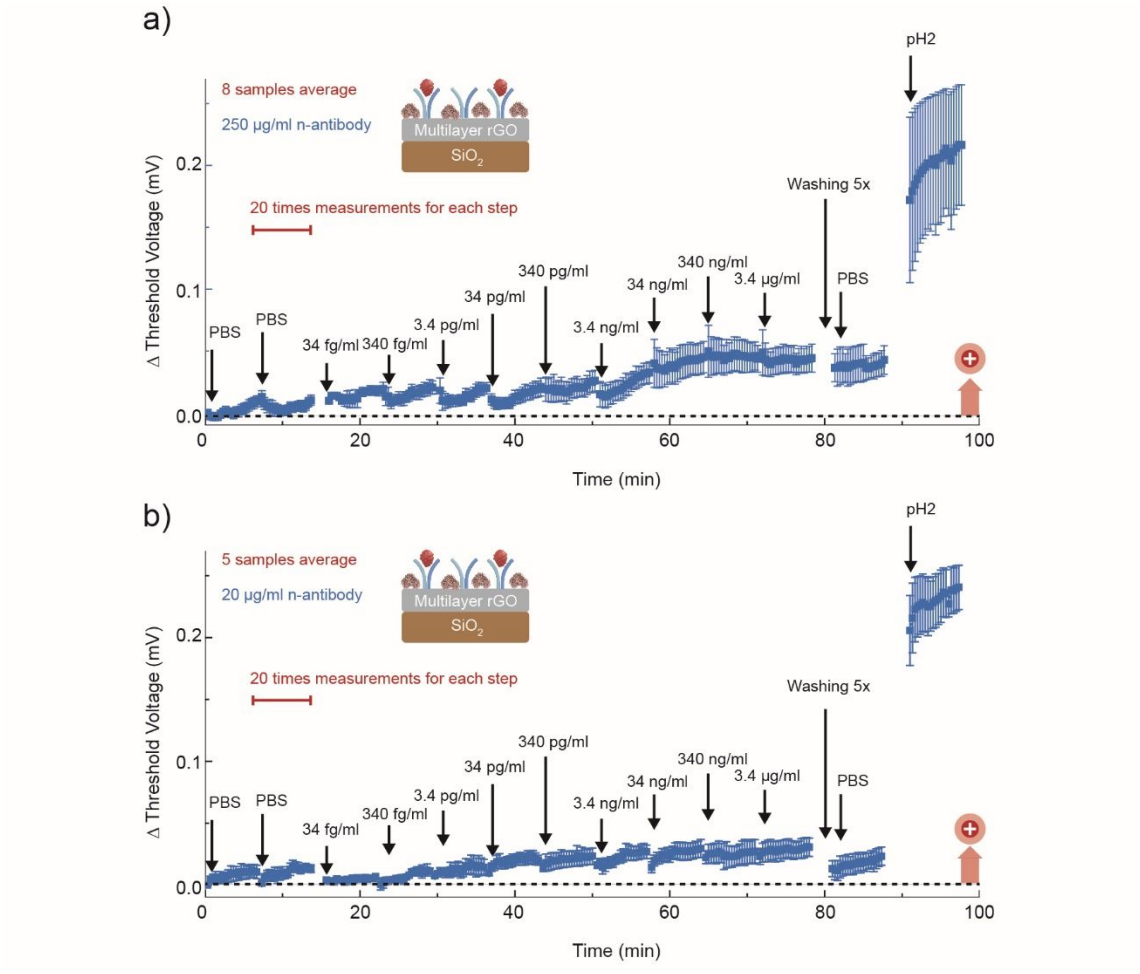

Figure S21. ΔV_{th} distributions of rGO layers functionalized with (a) 250 and (b) 20 μg/ml n-antibodies for increasing S proteins from 34 fg/ml to 3.4 μg/ml over time; each ΔV_{th} in the same measurement condition was averaged from 8 and 5 samples of rGO in a different batch, respectively. At the end of the S protein detection, the remote FG surfaces were washed five times with a pure PBS solution and then sequentially measured in a pure PBS media again to confirm the remaining signals between the antibody and the spike protein. After measuring the remote FG surfaces in a PBS solution, the pH2 solution was measured using the same FG surface. A sharp shift at pH2 resulted from changes in surface potentials on rGO in responding to pH changes, indicating the presence of rGO layers even after all the biosensing experiments.

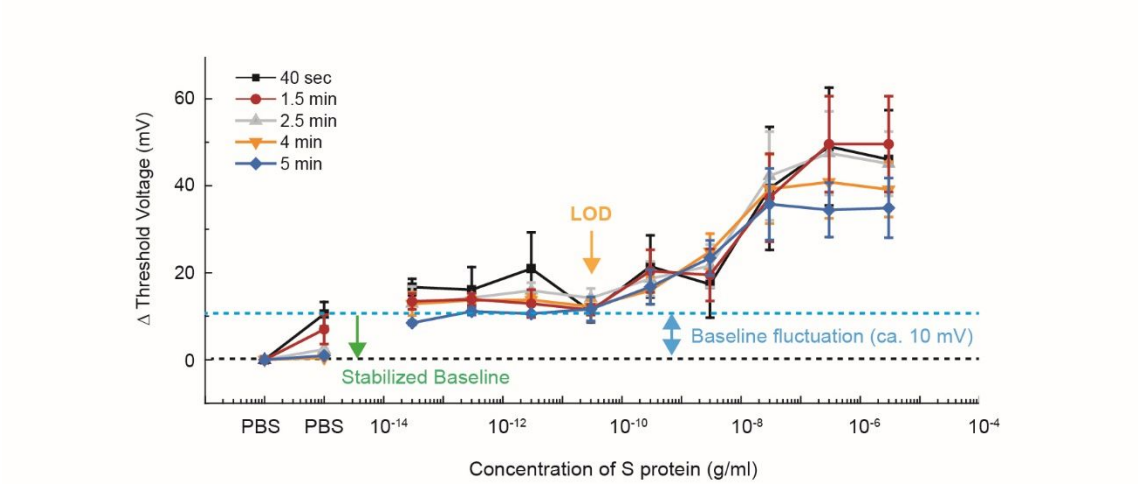

Figure S22. ΔV_{th} levels of 250 μg/ml antibody-functionalized rGO in response to S protein concentrations but obtained from different intervals of measurement time in a range from 40 sec to 5 min. Stabilized baseline and ΔV_{th} sensing curves began to show ΔV_{th} taken after at least 2.5 min measurements. A large difference in baseline, however, was observed from ΔV_{th} taken after the measurements with less than 2.5 min. This suggests that for the early stage of measurements, drift effects in V_{th} and signal fluctuation significantly surged but soon stabilized after some measurement time around reaching quasi-equilibrium. Therefore, longer measurement time of 5 min was chosen to obtain stable ΔV_{th} levels in quasi-equilibrium, which could minimize the impact of measurement time and drift on sensitivity of devices. It is noted that the maximum fluctuation in baselines that could occur for any measurement conditions is measured to be ca. 10 mV as shown in Figure S22. Thus, conservative LODs could be determined at the concentration of S protein showing ΔV_{th} above 10 mV.

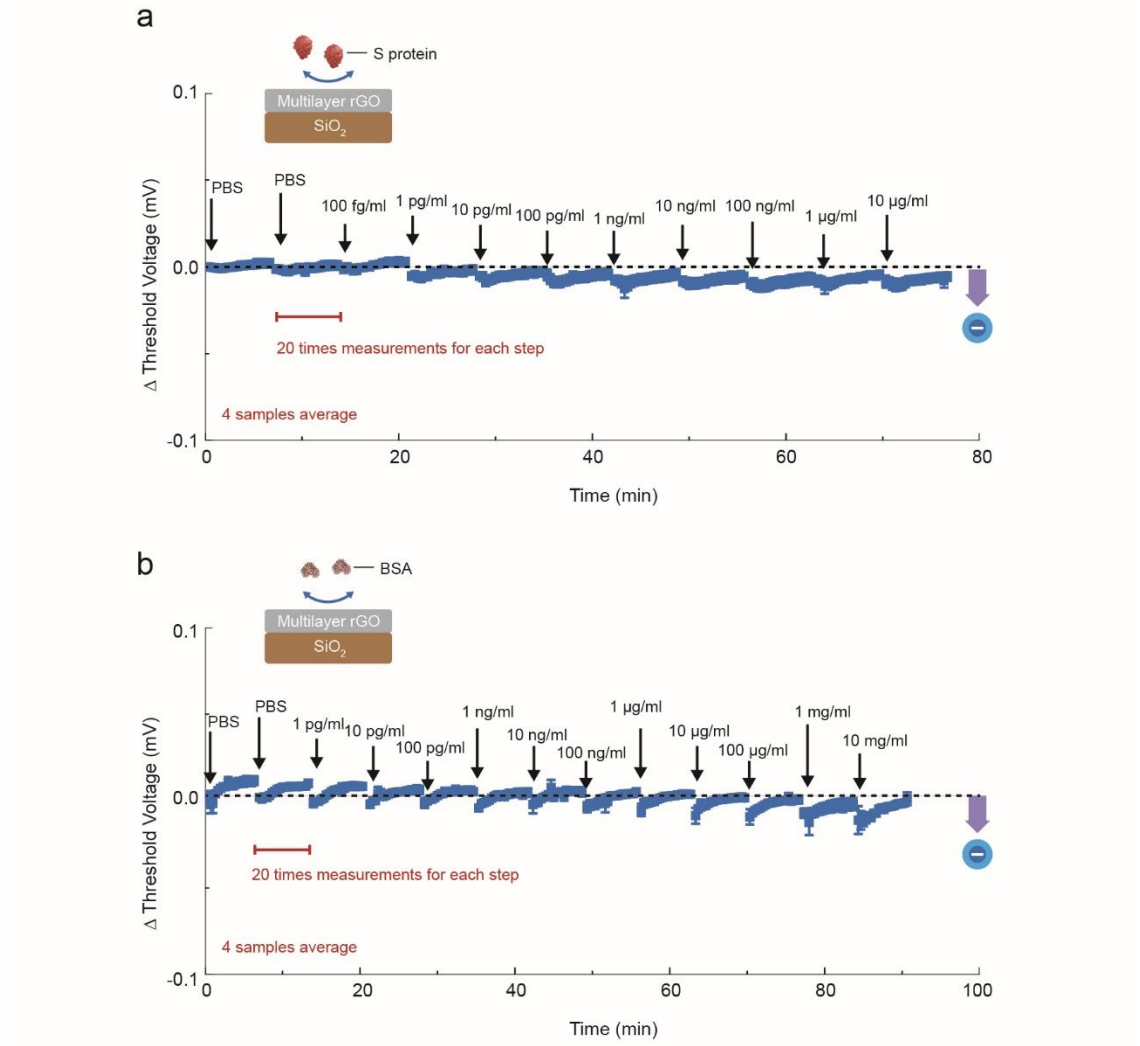

Figure S23. ΔV_{th} distributions of bare rGO layers for increasing (a) S proteins in a range from 100 fg/ml to 10 μg/ml over time and (b) BSA concentrations in a range from 1 pg/ml to 10 mg/ml.

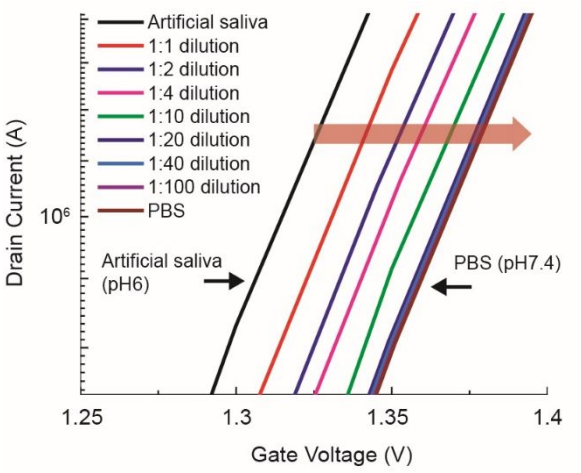

Figure S24. Transfer curves of a bare rGO surface measured in a pure artificial saliva, artificial saliva mixtures with different dilution ratios between artificial saliva and 0.05 × PBS, and a pure 0.05 × PBS. For artificial solution mixtures, the pure artificial saliva at pH 6 was diluted in a 0.05 × PBS solution at pH7.4 with a different ratio of the PBS solution. Transfer curve of the artificial solution mixture diluted in a ratio of 1:20 (artificial saliva:PBS) is mostly overlapping with that of a pure 0.05 × PBS, implying that the pH value of both the artificial solution mixture and the 0.05 × PBS was controlled at 7.4.